International Journal of Engineering Trends and Technology
ISSN: 2231 – 5381 /doi:10.14445/22315381/IJETT-V70I1P234
Volume 70 Issue 1, 291-298, January, 2022

Comparison of Mechanical properties in Single-Pass, Two-Pass and Three-Pass approach Friction Stir Processing of Aluminium Alloy

Sukhvir Yadav[1], Sanjeev Sharma[2], Bhupender Singh[3], P.B. Sharma[4]

[1]*Research Scholar Department of Mechanical Engineering, Amity University, Gurugram, India, 122 413*
[2]*Associate Professor, Department of Mechanical Engineering, Amity University, Gurugram, India, 122 413*
[3]*Assistant Professor, Department of Mechanical Engineering, J C Bose University of Science and Technology, Faridabad, India, 121 006*
[4]*Vice-Chancellor, Amity University, Gurugram, India, 122 413*

[1]sukhvirlisana@gmail.com, [2]ssharma26@ggn.amity.edu, [3]bhupee_28@yahoo.co.in

***Abstract* —** *The present work has been carried out to utilize the microstructural modification advantage given by Friction Stir Processing (FSP) on an AA6082-T6 metal system of 10mm thick. In the last decade, varying the number of passes on various aluminium alloys FSP has grabbed the attention of many researchers. The main focus of studies was on altering the number of passes, choosing the advancing side (AS) or Retreating side(RS) of tool movement, as well as varying overlapping ratios. In the present work, the authors considered one pass, two passes, and three pass approaches with 100% overlapping and advancing side tool movement. Surface morphology was analyzed through an optical microscope (OM) and scanning electron microscopy (SEM). The process was analyzed for tensile strength, percentage elongation, and proof stress. The study revealed that although the three-pass approach leads to better grain refinement yet, the single-pass approach resulted in higher tensile strength and comparative percentage elongation of the FSPed sample. Additionally, tool wear was also reported lesser in the single-pass approach in comparison to others.*

Keywords — *Grain refinement, Multipass, Tensile strength, Tool wear.*

I. INTRODUCTION

During the last decade, extensive research has been carried out on the FSP technique in comparison to other SPD (Severe Plastic Deformation) techniques. Being evolved out from Friction Stir Welding (FSW), FSP has an upper edge due to improvement in micrographs and ultimately enhancement of mechanical properties of the work piece. The heat generated in FSP leads to softness in grain structure along the machining side (Stir Zone). In conventional FSP, sometimes tunnel defect is reported in the FSPed sample. To eliminate tunnel defects, multi-pass tool movement was adopted[1]. In most of the studies, single-pass FSP was adopted[2–4], and stir zone is prepared by the single-pass approach, which is the prominent reason for tunnel defect[5]. Ramesh *et al.*[6] performed FSP by dual techniques, i.e., CMP (continuous multi-pass) FSP and IMP (intermittent multi-pass) FSP. It was observed that the IMP process showed better microstructure and high ductility. Gandra*et al.*[7] observed the superimposing by AS direction and by the RS direction for defect of overlapping and concluded that the AS side leads to a more uniform thickness layer in comparison to RS.

Aluminum Alloy 6082 T6, artificially aged, is a structural alloy of numerous industrial importance like aerospace, automotive industries, shaping, etc. The machining on Al-6082 T6 provides moderate results due to the higher composition of manganese (Mg) present in the grain structure. The FSP is the most convenient machining technique to improve grain structure as well as tensile strength. Unlike to conventional single-pass approach, Madgi. *et al.*[8] analyzed the three passes 100% overlapping on variable transverse speeds and observed that as we increase the number of passes, there will be increment in misorientation angle. Senthil Kumar. *et al.* [9] found the elimination of tunnel defect on multi-pass Al 6082 by 100% overlapping but the reduction in ultimate tensile strength (UTS) at stir zone due to high heat accumulation. Muribwathoho*et al.* [10] observed the performance of multi-pass FSP on comparatively weaker base material on AS for enhanced percentage elongation but low UTS. Zykona. *et al.*[11]reviewed the FSP on different alloys, and Al 5086 alloy loosened the strength in multi-pass as that of base metal. Mustafa. *et al.* [12] also reviewed the effect of multi-pass FSP on tensile strength for metallic alloys and metal matrix(MMCs) composites and concluded with the fact that mechanical properties of metallic alloys can be improved in selected reasons only while slight enhancement in MMCs during multiple passes.

In this work, IMP FSP with 100% overlapping is investigated considering three different FSP passes approaches, namely single pass, two-pass, and three-pass. The grain refinements along SZ are evaluated by optical microscope analysis, and SEM analysis is carried out to investigate the orientation of grain boundaries in a single pass, two passes, and three passes about base material along with the AS FSPed specimens. In addition to this tensile testing and percentage, elongation is compared in these three approaches. The process parameters, namely tool transverse speed, rotational tool speed, and numbers of passes, are selected for experimentation by the response surface method (RSM) technique (L_{20} array).

II. MATERIAL AND METHOD

A. Friction Stir Processing

As per the response surface method (RSM) L_{20} array, samples of size 300mmx 25mm 10mm thickness were cut longitudinally in plate shape was chosen. The specimens were undergone normal cleaning before the actual process. The specimen was fixed in a specially designed fixture on a vertical milling centre (sigma make) for processing, as shown in Fig.1. Commercial aluminium alloy 6082-T6 was used as the base material. Different constituents of Al 6082-T6 are mentioned in Table-1. The non-consumable D2 steel tool, octagonal-shaped 6.5mm pin height and 20mm shoulder diameter, was selected as a tool as shown in Fig. 2. The tool was mounted perpendicularly. The processing parameters were set on a machine provided by response surface methodology L_{20}array.FSP was carried out on these specimens at atmospheric conditions, i.e., at room temperature.

TABLE I. Al-6082 T6 CHEMICAL COMPOSITION

Element	% Present
Si	0.6-1.2
Mg	0.5- 1.3
Mn	0.3-1.1
Fe	0.0-0.6
Zn	0.0-0.3
Ti	0.0-0.2
Cu	0.0-0.2
Cr	0.0-.025
Al	Balance

Figure 1: Vertical Milling Machine

Figure 2: Hexagonal tool pin

The experimentation was performed on this setup as per the following RSM L_{20} array, as shown in Table 2.

Table II. L_{20} Array

Run	Factor-1	Factor-2	Factor-3
	Tool Rotational Speed (rpm)	Tool traverse Speed (mm /min.)	Number of Passes
1	1450	84	3
2	1190	65	2
3	930	43	3
4	1190	65	2
5	1190	65	2
6	930	43	1
7	1450	65	2
8	930	65	2
9	1450	84	1
10	1450	43	3
11	930	84	3
12	1190	65	2
13	1450	43	1
14	1190	43	2
15	1190	65	3
16	1190	84	2
17	930	84	1
18	1190	65	1
19	1190	65	2
20	1190	65	2

B. Microstructural Characterization

Microstructure analysis was carried out on a 2D optical microscope. The samples were machined on the processed region of the required dimension, i.e. 25mmx10mm, thickness 2mm, in strip form. For revealing complete surface morphology, Keller's etchant was used to clean the processed surface. Electropolishing was applied to get a mirror-like image. Scanning Electron Microscopy (SEM) analysis was obtained using Zeiss EV 50 (Resolution capacity- 2.0nm@30KV, Acceleration voltage- 0.2-30KV), and the specimens of requisite dimension, i.e. 10mm square, were gold coated before analysis. It was used for examining the grain morphology and precipitation process on the processed material.

C. Mechanical Testing

For calculating tensile strength, proof stress and percentage elongation specimens were prepared in dumbly shaped of size120 mm x 15 mm x 8 mm, thickness 6mm, cut along dwell surface as shown in Fig. 3 from the processed region. 20 samples were tested on UTM of 20 KN capacity at ambient temperature. The range was set between 0-6KN for examining the above-mentioned material properties. Hardness values for the processed region, with a gap of 0.5mm for either side from the stir zone, were calculated by Vicker's hardness tester by putting a load of 300 gf for a single pass, two passes, and three passes processed region.

Figure 3: Dumbly shaped cut along dwell surface for UTM

III. RESULTS AND DISCUSSION

A. Tensile Strength, Proof strength, and Percentage elongation analysis

The fractured tensile specimens as shown in Fig. 4. and their results illustrate that single pass, high rotational speed i.e1450 rpm, and high tool transverse speed i.e., 84 mm/min, resulted in the largest value of tensile strength (TS). Unlike to single pass and tool rotational speed and tool transverse speed ratio, the three-pass approach resulted in a considerable decline in TS on the same parameters as that of a single pass. The comparison of TS and % age elongation is translated in Table-3.

TABLE III. MECHANICAL PROPERTIES OF SPECIMENS

Run	Tensile strength (N/mm^2)	0.2% proof strength/ Yield strength (N/mm^2)	% Elongation GL=50mm
1	186	111	10.5
2	171	114	18.5
3	169	120	18.5
4	171	114	18.5
5	171	114	18.5
6	169	107	15.0
7	182	106	18.4
8	184	104	16.5
9	196	104	14.0
10	172	96	14.0
11	174	115	15.5
12	171	114	18.5
13	186	107	15
14	181	113	19
15	174	112	18
16	183	110	16.5
17	185	108	10.5
18	183	118	14.5
19	171	114	18.5
20	171	114	18.5

Figure 4: Fractured Specimens after UTS Testing

Likewise, % age elongation of single-pass was also 40% higher than that of three passes, while the two-pass peak TS (Specimen number 8 TS- 184) had the highest % age elongation, which is 15% higher than single-pass peak TS specimen (Specimen number 9, TS- 196). The load extension curves also illustrated the same as indicated supplementarily.

B. Micro Structural Analysis

Three tensile strength peak specimens of each approach (Specimen no. 9 – single pass, 8-2 pass, 1-Three pass) were selected for microstructural analysis. The three-pass specimen (number-1) showed the highest homogenous and void-free structure, as shown in the figure. 5(c). The Tunnel cavity along SZ was nearly eliminated in this sample while at lower rotational speed in three passes was still producing the same defect. The same rpm/ωratio for single-pass resulted in improved microstructure but not tunnel void-free. The main cause of the result indicated that FSP influences on given structure recrystallization and lowers the tunnel voids at a higher rpm/ω ratio.

Figure 5(a): Single- Pass test specimen

Figure 5(b): Two-Pass test specimen

Figure 5(c): Three- Pass test specimen

It was found that increment in the number of passes and process rpm/ω ratio in FSP leads to tunnel void dismissing, which has been depicted in fig. 6(a), 6 (b), 6 (c). On the other hand, by increasing these parameters, mechanical properties, namely TS and % age elongation, are compromised for a structural component. Therefore, single-pass, 100% overlapping, advancing side-tool motion, and higher rpm/ω ratio may provide desirable mechanical properties to AA 6082 T6.

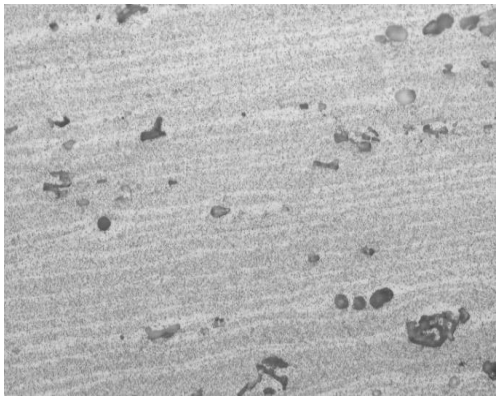

Figure 6(a): Single-Pass Specimen Microstructure

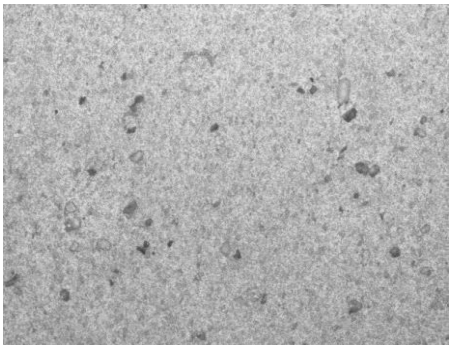

Figure 6(b): Two-Pass Specimen Microstructure

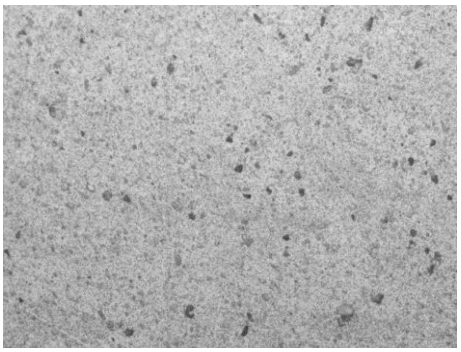

Figure 6(c): Three-Pass Specimen Microstructure

C. SEM Analysis

SEM images of base metal (BM) at three different magnifications are depicted in Fig. 7(a)-7(c). contains highly elongated aluminium grains. The coarser grain size of BM converts into the fine structure of the FSPed surface, and it happened because of heat generation, which resulted in plastic deformation of the processed part of the work piece. The second phase particles in the BM and FSPed surface are found in strip and rod shapes [1]. It was observed that the size of the strip shape particles in BM was larger than that of the rod shape, and in the FSPed surface, it was reversed. The strip shape is shown as A and rod as B in BM. The severe plastic deformation causes a reduction in the size of the strip hence reduction of density. The strip shape particles are iron-based, while rod-shaped are silicon-based particles. In BM, the small continuous round-shaped particles found along the grain boundaries are silicon-based particles and are shown as C in figure 7(b). These particles hinder the grain boundary migration, resulting in an increase in strength.

SEM micrographs of single-pass, two-pass and three-pass are shown in Fig. 8(a)-8(c), 9(a)-9(c) and 10(a)-10(c) respectively. The transformation of BM micrographs into new material structured micrographs is seen. Due to the dynamic recrystallization of the BM, fine equiaxed aluminium grains were obtained. The continuous layer as in BM of silicon particles becomes discontinuous in the FSPed surface. In the FSPed sample, iron-based (point D) and silicon-based (point E) particles are present lesser in comparison to BM.

In the single-pass FSP process, high heat generation results in a lesser number of precipitates. These silicon and iron-based particles control the properties (mechanical properties) of the material. The iron-based particle structure converted into small grains resulted in a more fine and equiaxed structure. The finer grain structure resulted in more elongation than the base metal. The structure in Fig is shown as point F and point G. Two-pass FSPed specimen undergoes more heat generation resulting in more precipitation. These are shown as point H and point I in fig. More precipitation causes softening of material and more elongation. A three-pass FSPed specimen undergoes more changes than a two-pass and single pass. Due to continuous multipass high heat is generated during the process. As a result, the fine-grained structure changed into a coarser grain structure which resulted in lower strength of the material and less elongation. The precipitation process is shown as point J and points K.

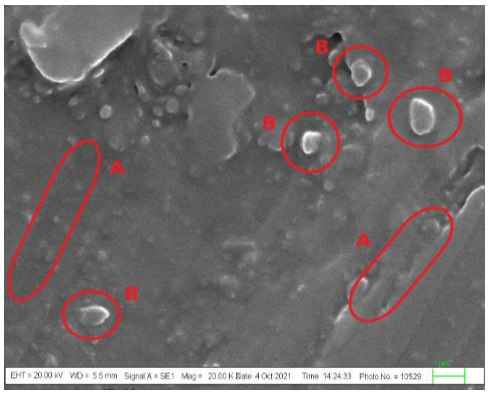

Figure 7(a): SEM image base material at 20.00K magnification

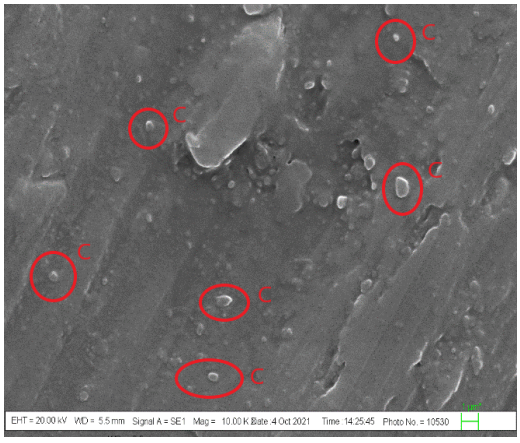

Figure 7(b): SEM image base material at 10.00K magnification

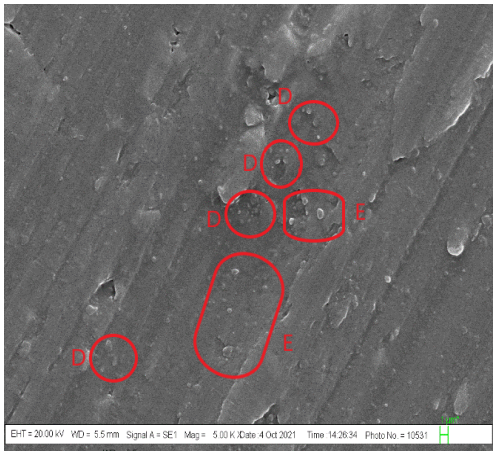

Figure 7(c): SEM image base material at 5.00K magnification

Figure 8(a): SEM image Single Pass at 20.00K magnification

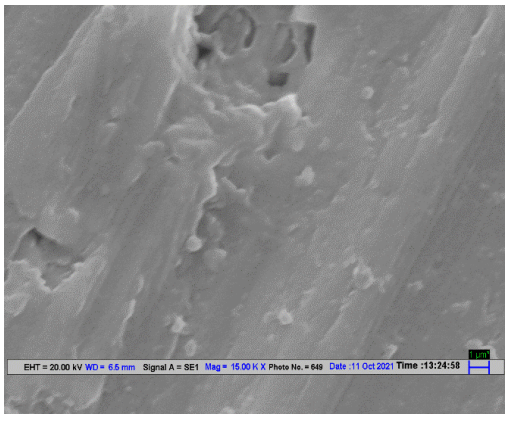

Figure 8(b): SEM image Single Pass at 10.00K magnification

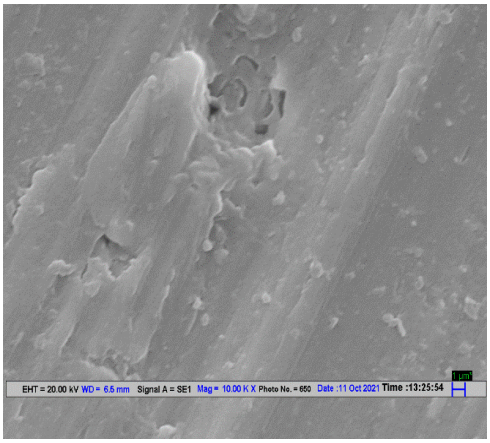

Figure 8(c): SEM image Single Pass at 5.00K magnification

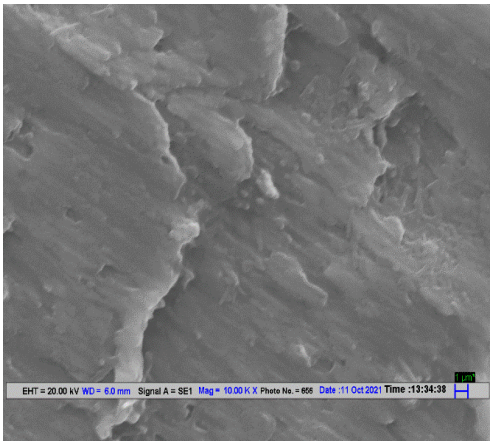

Figure 9(c): SEM image Two-Pass at 5.00K magnification

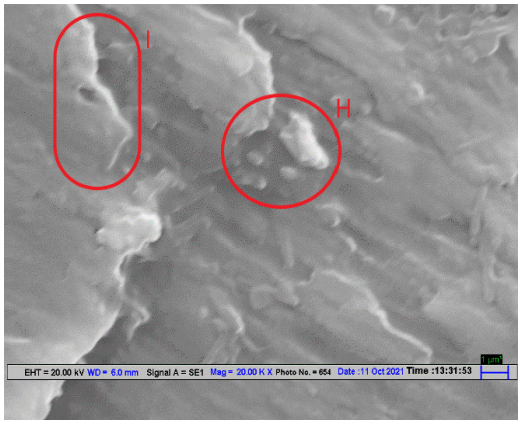

Figure 9(a): SEM image Two-Pass at 20.00K magnification

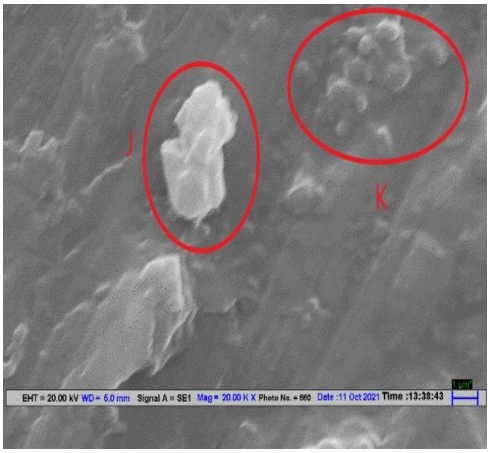

Figure 10(a): SEM image Three Pass at 20.00K magnification

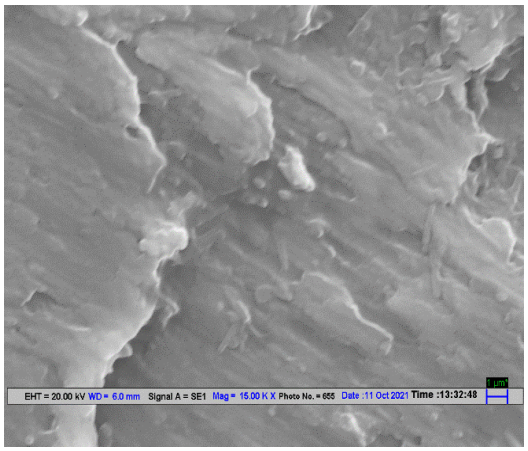

Figure 9(b): SEM image Two-Pass at 10.00K magnification

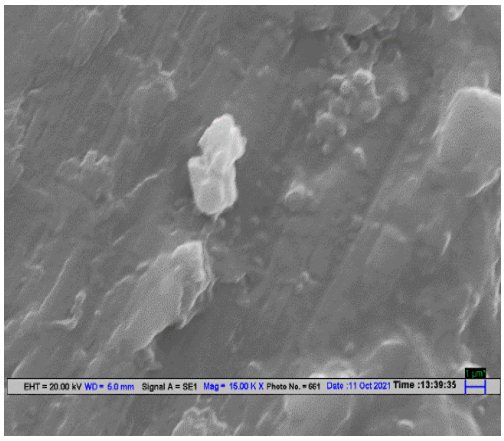

Figure 10(b): SEM image Three Pass at 10.00K magnification

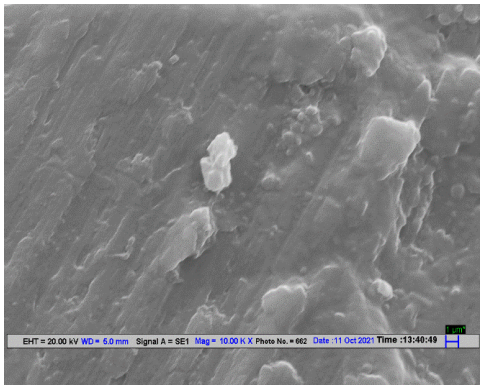

Figure 10(c): SEM image Three Pass at 5.00K Magnification

D. Microhardness Analysis

Hardness graphs for single-pass, two passes, and three passes are shown in Fig. 11(a)-11(c), respectively. It is revealed from the graphs that the microhardness value for single-pass 52.7HV is slightly higher than three pas 51.5HV. Hardness values in the advancing side are somewhat higher than the retreating side. Moreover, hardness is uniformly distributed along the stirred zone.

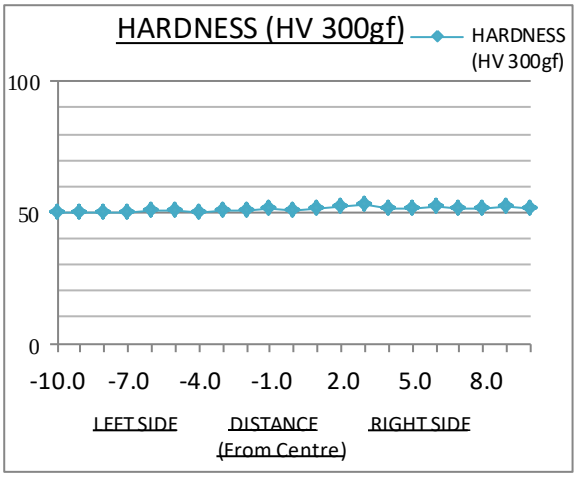

Figure 11(a): Microhardness graph for single pass

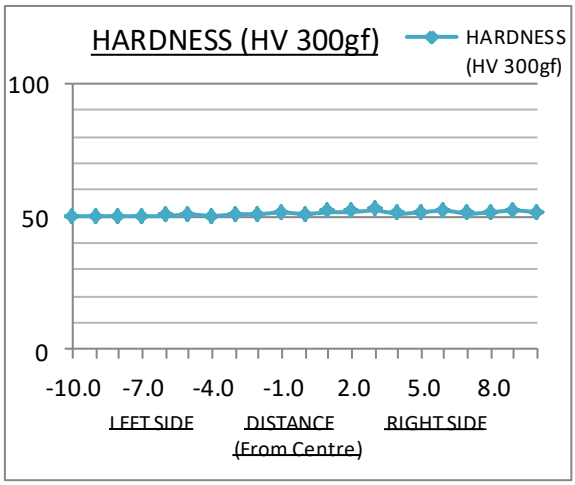

Figure 11(b): Microhardness graph for two-pass

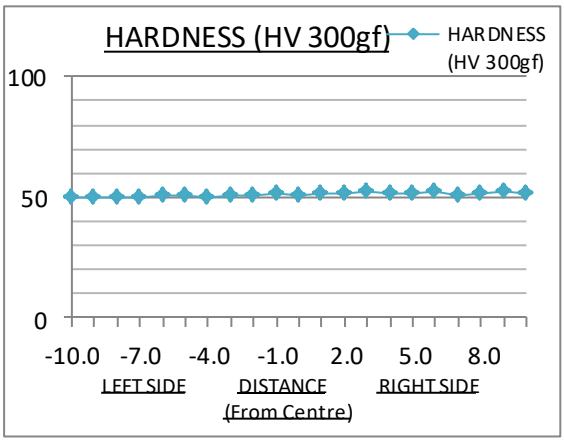

Figure 11(c): Microhardness graph for three passes

IV. CONCLUSIONS

FSP was carried out on Al 6082 T6 by three different pass approaches, AS, 100% overlapping on different process parameters. The TS, % age elongation and microstructural analysis have been investigated along SZ. The following conclusions were drawn:

I. Three pass approaches with the same rpm/ω ratio as that of the single-pass have limited scopes of TS improvement, while the single-pass approach resulted in the highest TS among the whole array model.

II. Although the single-pass specimens, % age elongation is slightly lower than two pass approaches, it is 40% higher than three pass FSP. So single-pass approach is suitable due to lesser machining time and highest tensile properties.

III. High heat accumulation and material softening resulted in tunnel void-free FSPed sample in three pass approaches, but the material softening may cause alternating material in structural applications.

IV. Tool wear was also reported to a lesser extent for single-pass as compared with two-pass and three-pass approaches.

ACKNOWLEDGMENT

The author would like to acknowledge the CRF lab at IIT Delhi and M/s. Sunbeam Lightweighting Solutions Private Limited for their valuable support in material testing. The author would also like to thank M/s. Authentic Engineers Private Limited for providing base material in such a short period

REFERENCES

[1] M.V.N. V Satyanarayana, K. Adepu, K. Chauhan, Effect of Overlapping Friction Stir Processing on Microstructure, Mechanical Properties and Corrosion Behavior of AA6061 Alloy, Met. Mater. Int. (2020). https://doi.org/10.1007/s12540-020-00757-y.

[2] H. Zhao, Q. Pan, Q. Qin, Y. Wu, X. Su, Materials Science & Engineering A Effect of the processing parameters of friction stir processing on the microstructure and mechanical properties of 6063 aluminium alloy, Mater. Sci. Eng. A. 751 (2019) 70–79. https://doi.org/10.1016/j.msea.2019.02.064.

[3] K.J. Al-Fathallah, A.I. Almazrouee, A.S. Aloraier, Microstructure and mechanical properties of multi-pass friction stir processed

aluminium alloy 6063, J. Mater. (2013). https://doi.org/10.1016/j.matdes.2013.07.062.
[4] I. Charit, R.S. Mishra, High strain rate superplasticity in a commercial 2024 Al alloy via friction stir processing, 359 (2003) 290–296. https://doi.org/10.1016/S0921-5093(03)00367-8.
[5] K. Elangovan, V. Balasubramanian, Materials & Design Influences of tool pin profile and tool shoulder diameter on the formation of friction stir processing zone in AA6061 aluminium alloy, 29 (2008) 362–373. https://doi.org/10.1016/j.matdes.2007.01.030.
[6] K.N. Ramesh, S. Pradeep, V. Pancholi, Multipass Friction-Stir Processing and its Effect on Mechanical Properties of Aluminum Alloy 5086, 43 (2012). https://doi.org/10.1007/s11661-012-1232-3.
[7] J. Gandra, R.M. Miranda, P. Vilac, Effect of overlapping direction in multipass friction stir processing, 528 (2011) 5592–5599. https://doi.org/10.1016/j.msea.2011.03.105.
[8] M.M. El-Rayes, E.A. El-danaf, Journal of Materials Processing Technology The influence of multi-pass friction stir processing on the microstructural and mechanical properties of Aluminum Alloy 6082, J. Mater. Process. Tech. 212 (2012) 1157–1168. https://doi.org/10.1016/j.jmatprotec.2011.12.017.
[9] R. Senthilkumar, M. Prakash, N. Arun, A.A. Jeyakumar, PT US CR, Appl. Surf. Sci. (2019). https://doi.org/10.1016/j.apsusc.2019.06.132.
[10] O. Muribwathoho, V. Msomi, S. Mabuwa, S.S. Motshwanedi, Materials Today : Proceedings Impact of multi-pass friction stir processing on microhardness of AA1050 / AA6082 dissimilar joints, Mater. Today Proc. (2020) 2–8. https://doi.org/10.1016/j.matpr.2020.11.587.
[11] A.P. Zykova, S.Y. Tarasov, A. V Chumaevskiy, E.A. Kolubaev, A Review of Friction Stir Processing of Structural Metallic Materials : Process, Properties, and Methods, (2020) 1–35. https://doi.org/10.3390/met10060772.
[12] E. Moustafa, S. Mohammed, S. Abdel-wanis, Review Multi-Pass Friction Stir Processing, (n.d.) 98–108.